Microstructure/Mechanical Property Relationship in a DS Cast Ni_3Al-Base Alloy

Y.F. Han, Y.M. Wang, and M.C. Chaturvedi

A Ni-Al-Mo directionally solidified (DS) casting γ'-base superalloy, with the chemical composition (wt%) 7.5 to 8.5% Ni, 10 to 14% Al, Mo ≤0.15% B, has been developed for advanced gas turbine blades and vanes. The mechanical properties of this alloy have been determined by tensile tests at room temperature and in the temperature range 700 to 1000 °C and by stress-rupture tests in the temperature range 760 to 1100 °C. The microstructures of the as-cast and homogenized specimens and of specimens after creep deformation at 1000 to 1100 °C have been examined by scanning electron microscopy (SEM), transmission electron microscopy (TEM), and optical microscopy techniques. The results show that this alloy has a high yield strength from room temperature up to 1100 °C, excellent creep resistance at temperatures up to 1100 °C, as well as a lower density and higher melting point than currently available nickel superalloys. The microstructural observations and analysis indicate that the superior mechanical properties of this alloy may be attributed to solid solution hardening by the large molybdenum addition, second-phase strengthening by γ phase and other minor phases that precipitate in various temperature ranges, the formation of a γ raft structure during creep, and to the existence of high-density misfit dislocation networks at γ'/γ interface areas due to a high value of γ'/γ misfit.

Keywords
creep, microstructures, misfit dislocations, Ni_3Al, strengthening mechanism, yield strength

1. Introduction

AT present, most of the gas turbine blades and vanes of advanced aeroengines are made of nickel-base superalloys. With the development of aeroengines for high-performance aircraft, the operating temperatures of these parts are constantly increasing, which limits the use of nickel superalloys. In addition, the high density and need to use expensive alloying elements, such as hafnium, tantalum, and rhenium, has caused the search for new materials, some of which are based on intermetallic compounds. As a matrix for superalloys, Ni_3Al has some inherent advantages,[1-3] such as high melting point, low density, high resistance to oxidation, low coefficient of diffusion, high resistance to elevated temperature creep, and a yield strength that increases with increasing temperature up to 800 °C. However, the strength of single-phase Ni_3Al, including alloyed Ni_3Al solid solution, is considerably lower than that of two-phase nickel-base superalloys. One method of improving the strength of Ni_3Al is by introducing a second phase via one of the following methods: (1) the *in situ* formation of γNi solid solution or βNiAl phase by adjusting the composition to alter the ratio of nickel and nickel site occupying elements to aluminum and aluminum site occupying elements; (2) the formation of second-phase particles such as carbides and borides by the addition of appropriate elements; and (3) the addition of second-phase particles or fibers such as TiC, HfC, TiB_2, Al_2O_3, and Y_2O_3 by special processing techniques. Many two-phase γ'-Ni_3Al-base superalloys have been developed during the last 20 years[3-9] using these methods. They are either high-strength wrought alloys used in the intermediate temperature range of 650 to 900 °C or casting superalloys used at 1050 to 1100 °C. A high-performance casting γ'-base superalloy containing 14 wt% Mo, 7.8 wt% Al, 0.03 to 0.15 wt% B, and the balance Ni has been recently developed for the turbine blades and vanes of advanced aeroengines. The results of a study on microstructure/mechanical property relationships of this alloy are presented in this article.

Y.F. Han and **Y.M. Wang,** Institute of Aeronautical Materials, Beijing 100095, China; and **M.C. Chaturvedi,** Department of Mechanical and Industrial Engineering, University of Manitoba, Winnipeg, Manitoba, Canada R3T 2N2.

2. Experimental Techniques

The material used in the present investigation was unidirectionally cast Ni_3Al-base superalloy with a composition (wt%) of 7.8Al-14Mo-0.05B-bal Ni. The master alloy was prepared by a vacuum induction furnace at the refining temperature of 1570 to 1600 °C for 15 to 20 min. The columnar grain rods for tensile and creep tests were produced by a rapid solidification method in a commercial DS vacuum induction furnace. The drawing rate of the Al_2O_3 precision investment mold filled with molten alloys and connected to a water cooling copper plate was 6.2 mm/min. The as-cast rods were then homogenized in a vacuum furnace at 1260 °C for 10 h. The rods were always oil quenched from the homogenizing treatment temperature to produce optimum properties. The tensile and stress-rupture tests were conducted on 5-mm diam. specimens with a gage length of 25 mm. The room-temperature and high-temperature tensile tests were carried out on an Instron universal testing machine at a strain rate of $3.3 \times 10^{-4}\ s^{-1}$ with the testing temperature controlled within ±3 °C. The stress-rupture tests were carried out by using constant-load creep machines in air

Table 1 Tensile properties of DS γ′-base alloy with the composition (wt%) of 7.8Al-14Mo-0.05B-bal Ni after 1260 °C/10 h followed by oil quenching

Tensile property	Testing temperature, °C						
	RT	700	760	870	1000	1050	1100
σ_{UTS}, MPa	1115	1040	1170	1075	705	585	465
	1225	1090	1165	1040	720		500
$\sigma_{0.2}$, MPa	805	980	1105	975	565	520	385
	780	995	1110	950	640		395
Elongation, %	14.2	8.5	6.3	11.0	28.1	28.0	44.0
	15.7	8.7	4.2	10.3	25.0		32.4

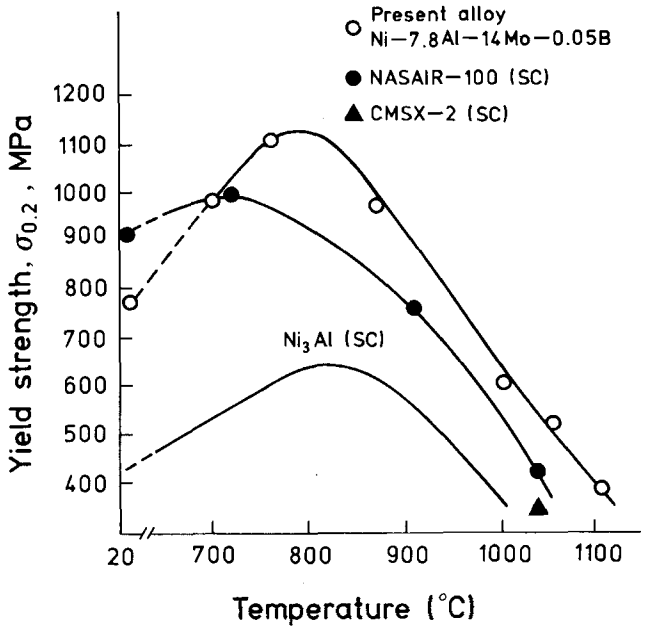

Fig.1 Variation in yield strength with temperature for the alloy used in this study, Ni_3Al single-crystal, nickel-base single-crystal alloy CMSX-2, and NASAIR-100.

at 760 to 1100 °C, with the testing temperatures controlled within ±3 °C.

The microstructural analyses of various specimens were conducted by optical, scanning, and transmission electron microscopy. The volume fractions of various phases were determined by quantitative image analysis using a Leitz Image Analyzer. The chemical compositions of phases larger than 2 μm were determined by X-ray energy-dispersive spectroscopy (EDS) and wavelength-dispersive spectroscopy (WDS) techniques using the polished surface of the specimens in a JXA-840 scanning microanalyzer. The chemical compositions of phases smaller than 2 μm were determined by X-ray EDS in a JEOL 2000 FX transmission electron microscope. The thin foils for TEM study were prepared by ion beam thinning 20 to 30 μm thick specimens in a Dual Ion Mill with an acceleration voltage of 6 kV at an angle of 15° for 4 to 6 h.

The lattice parameters of γ′ and γ phases at room temperature were determined by X-ray diffraction in an IBM-APD10 X-ray diffractometer using CuKα radiation at a voltage of 35 kV and a current of 35 mA. A step scanning method was used, and the scanning rate was 0.6 degrees/min with 0.02 degrees/step.

3. Results and Discussion

3.1 *Mechanical Properties*

Tensile tests were carried out at room temperature and in the temperature range of 700 to 1100 °C. The results are shown in Table 1. For comparison, the observed values of the tensile yield strength and those of single-crystal Ni_3Al and an advanced nickel-base single-crystal superalloy are shown in Fig. 1. The results in Table 1 and Fig. 1 show that the alloy used in this study has a higher tensile strength and a higher ductility. The tensile yield strength above 700 °C is higher than all commercial DS nickel-base superalloys and single-crystal alloys. Ductility at 760 °C, where a minimum in ductility occurs in most γ′/γ two-phase superalloys, is greater than 4%, which is acceptable for many engineering applications. Figure 1 also shows that the yield strengths of the alloys increase with temperature up to about 760 to 800 °C and then decrease with increasing temperature, as has been observed in other γ′-base alloys.

Stress-rupture tests were carried out at 760 to 1100 °C at various stress levels, and the results are shown in Table 2. For comparison, the stress-rupture lives of some advanced casting DS nickel- and Ni_3Al-base superalloys are also listed. DS NX 188 is an experimental γ′-base superalloy with a chemical composition (wt%) of Ni-18Mo-8Al-0.05C, which was developed in the early 1970s for gas turbine vanes operating at 1100 °C. PWA 1422 is a recently developed nickel-base superalloy (Ni-0.1C-Cr-10Co-12W-5Al-2Ti-1Nb-2Hf-0.02B-0.05Zr) widely used as turbine blade material for advanced aeroengines, and DZ-3 is a high-performance DS nickel-base superalloy (Ni-0.1C-11Cr-5Co-5W-4.2Mo-5.6Al-2.7Ti) developed in the 1980s at the Beijing Institute of Aeronautical Materials for use as gas turbine blade material. Table 2 shows that the creep resistance of the present Ni_3Al-base superalloy at an intermediate temperature of 760 °C and at higher temperatures of 1040 and 1100 °C is greater than these advanced experimental and commercial DS cast nickel-and Ni_3Al-base superalloys. The creep resistance of the alloy at 1040 to 1100 °C compares favorably with the advanced nickel-base single-crystal alloys CMSX-2 (Ni-8Cr-4.6Co-7.9W-0.1Hf) and NASAIR100 (Ni-9Cr-10.5W-1.0Mo-5.8Al-1.2Ti-3.3Ta). This is also illustrated in Fig. 2, which shows Larson-Miller parameter plots for 1038 and 1100 °C.[110] However, the density of the present alloy

Table 2 Comparison of stress-rupture lives of test alloy with advanced DS superalloys

Testing temperature, K	Stress level, MPa	Stress-rupture lives, h, for: Present alloy γ′ base	DSNX188 γ′ base	PWA1422 γ base	DZ-3 γ base
1033	804	197, >190	100	...	...
	765	190	...	100	...
1223	220	124, 122	...	...	...
	235	...	...	...	100
	255	...	...	100	...
1253	180	161-172	...	...	...
	206	...	...	100	100
1313	140	107-169	...	...	...
	137	...	...	100	100
1373	78.5	>667	30,39	...	100
	88.3	254	...	42,44	40,42
	100	115-188	...	...	...

(7.90 g/cm^3) is about 10% lower than that of CMSX-2 and NASAIR 100. Therefore, the density-compensated strength of this alloy is higher than these advanced single-crystal nickel-base alloys, which suggests that the present alloy has good potential for application in the manufacture of gas turbine components for use at 1000 to 1100 °C.

3.2 *Microstructure of the Alloy*

Typical microstructures in a specimen homogenized at 1260 °C for 10 h followed by oil quenching are shown in Fig. 3, which are the backscattered electron (BSE) images of the alloy obtained by SEM microscopy. According to the nickel-aluminum quasi-two-phase diagram with 8.2 at.% Mo shown in Fig. 4, the homogenization treatment at 1260 °C is in the γ + γ′ two-phase region. Therefore, a part of the as-cast γ′ phase remained in the homogenization heat treated specimen, as shown in Fig. 3. The results of EDS analysis indicate that three major phases—γ′, γ, and boride—are present in the homogenization heat treated condition. The white particles in area A in Fig. 3(b) are borides, the dark phase is γ′ - Ni_3 (Al,Mo) with a chemical composition of 74 to 75 at.% Ni, 21 to 22 at.% Al, 3.9 to 4.3 at.% Mo and the gray phase is γNi solid solution. Area A is the interdendritic area consisting of fine (0.1 to 0.3 μm) cubic-shaped γ′ phase with a skeletal network of γ phase around it and white particles of boride. Area B in Fig. 3(b) is the dendrite arm consisting of γ′ phase (1 to 2 μm) that did not dissolve by the homogenization treatment and a (γ′ + γ) two-phase area similar to area A. The volume fraction of γ′ phase in the present alloy was 75 to 80% as determined by quantitative image analysis.

The lattice parameters of γ′ and γ phases, as determined by X-ray diffraction, were found to be 3.5859 and 3.6289 Å, respectively. Therefore, the lattice misfit between the γ′ and γ phase is about 1.185%, which is higher than the reported values of lattice misfit in other nickel- and Ni_3Al-base superalloys. This high value of lattice misfit has been confirmed by the existence of high-density misfit dislocations in the area of γ′/γ interfaces, as shown in Fig. 5. Figure 5(a) was taken from a specimen homogenized at 1260 °C for 10 h, followed by oil quenching; Fig. 5(b) is the microstructure of a creep-deformed specimen showing misfit dislocation at the γ′/γ interface. It has been suggested that the generation of these interface dislocations is an irreversible process and that the system stabilizes itself by their creation.[11]

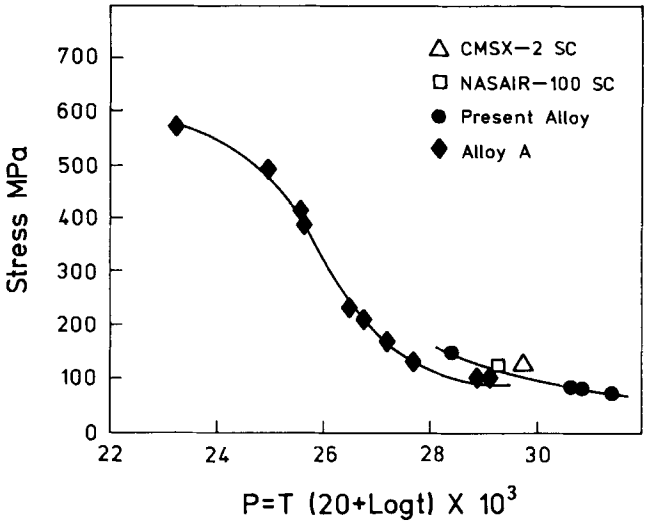

Fig. 2 Larson-Miller curves of the test alloy and other nickel-base DS and single-crystal (SC) alloys. *T* is testing temperature in K; *t* is stress-rupture life in hours.

The interface dislocations were found to be primarily edge dislocations. The Burgers vector of these interface dislocations was determined to be primarily $a/2\langle 110\rangle$ type and a very few were $\langle 100\rangle$ type. The interspace between two misfit dislocations, *d*, depends on the Burgers vector, **b**, and the misfit between the two phases, δ, and has been deduced by Brooks[12] to be equal to $\mathbf{b}/|\delta|$. The interspace of the nearest two misfit dislocations in the (100) interface was experimentally determined to be about 250 to 280 Å in the homogenization heat treated specimen, which is in good agreement with the value of 215 Å calculated using the lattice misfit value of 1.185% between γ and γ′. The difference in mesh size of the dislocation networks in the same area of the specimen, as shown in Fig. 5(a), may be attributed to the fact that the contrast of misfit dislocations observed in one crystal plane of thin foil, such as (001), arises not only from those dislocations in (001) plane, but also from other γ′/γ interface planes.

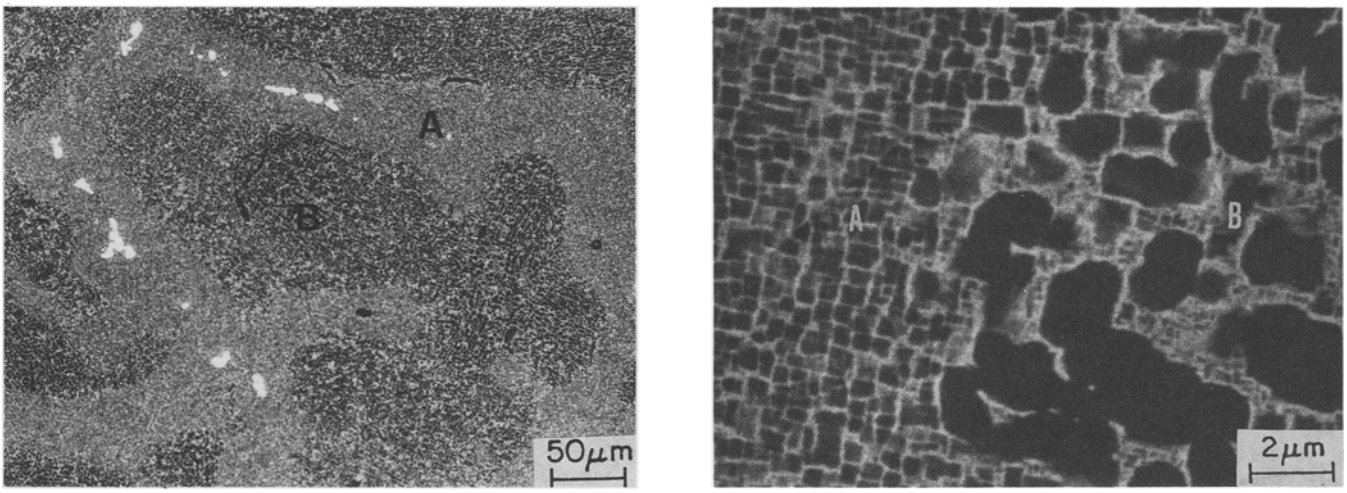

(a) (b)

Fig. 3 Backscattered electron images of the test alloy homogenized at 1533 K for 10 h and oil quenched. (a) Polished surface, showing areas A and B, and boride (white particle). (b) Higher magnification image of (a).

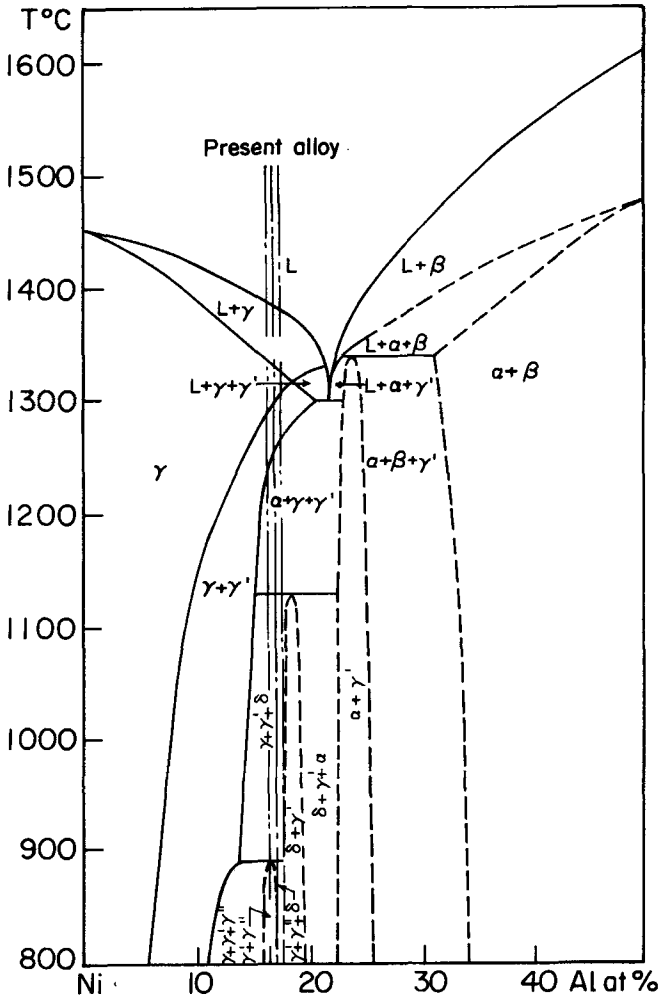

Fig. 4 Nickel-aluminum quasi-two-phase diagram with 8.2 at.% Mo.

3.3 *Microstructure/Mechanical Property Relationships*

The results of this study suggest that the alloy used in this investigation exhibits high tensile strengths up to 1100 °C and good creep resistance at both the intermediate and high temperature ranges. These properties, like those of any other complex alloy, are the result of a complex interplay of various strengthening mechanisms. In the present alloy, these mechanisms are likely to be (1) solid-solution strengthening by molybdenum of both γ' and γ phases, (2) second-phase strengthening of γ' by 20% volume fraction of γ and other minor phases, (3) the formation of raft structure during high-temperature creep, and (4) the presence of misfit dislocations networks at the γ'/γ interface, which can provide an effective barrier to dislocation motion. It is not possible to quantify the exact contribution by each of these mechanisms to the overall strength of the alloy; therefore, their origin and contributions will be discussed only qualitatively.

3.3.1 Solid-Solution Hardening by Molybdenum Addition

Molybdenum has been widely used as a strengthening element in many commercial nickel-base superalloys, because it can strengthen both the γ matrix and the γ' phases. Compared with other refractory elements such as tungsten, cobalt, tantalum, niobium, and hafnium, it has higher solubilities in both the γ and γ' phases. For example, the solubility of molybdenum in γNi is 21 at.% from room temperature to 800 °C and 36 at.% at 1260 °C. In γ'-Ni_3Al, its solubility is 6 to 8 at.%.[13,14] Because molybdenum has a larger atomic radius (r_{Mo} = 1.3625 Å) than γ'Ni (r_{Ni} = 1.2325 Å) but a smaller radius than Al (r_{Al} = 1.4315 Å), addition of molybdenum will cause lattice distortion of both the γ' and γ phases. This distortion can increase the resistance to dislocation motion and will also increase the activation energy for diffusion and creep processes, thus making the microstructure of the alloy relatively more stable at high temperature. The solubilities of molybdenum in the present al-

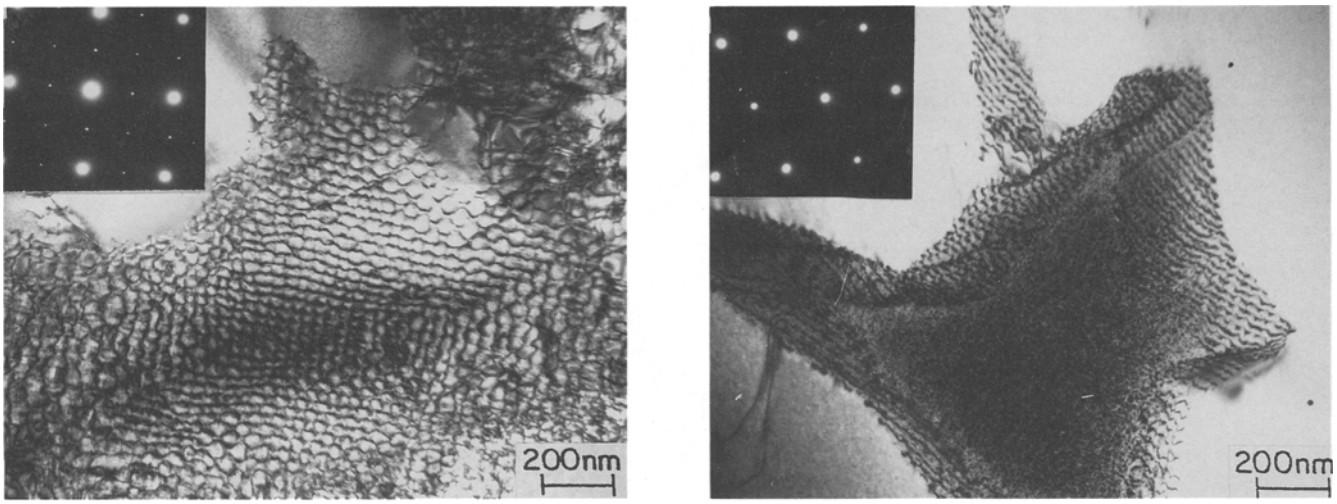

(a) (b)

Fig. 5 TEM micrographs showing misfit dislocation networks in specimen (a) homogenized at 1533 K for 10 h and oil quenched; and (b) after creep deformation at 1373 K/95 MPa, 190 h.

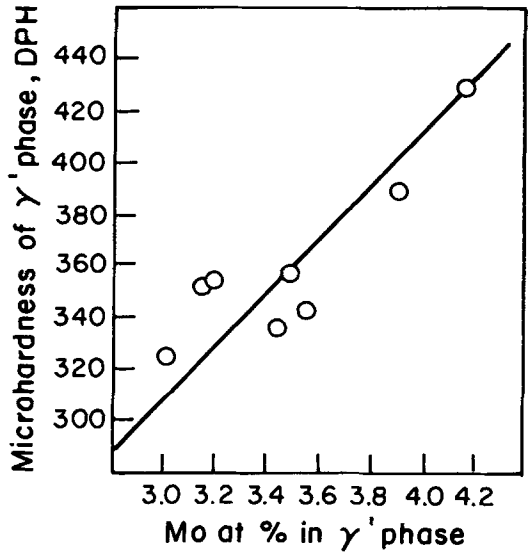

Fig. 6 Dependence of room-temperature hardness of γ phase on molybdenum content.

loy were found to be about 5.4 to 5.5 at.% in γ' and 15.2 to 15.9 at.% in the γ phase. Because the volume fraction of the γ' phase in the present alloy is about 80%, it is assumed that the strength of the γ' phase may be the main factor in determining the strength of this alloy. It has been reported[15] that both the 0.2% flow stresses of Ni_3Al at peak temperature and at −196 °C increase with an increase in molybdenum content. The strengthening effect of molybdenum on the γ' phase in the present Ni-Al-Mo alloy system has been empirically analyzed, and the results are shown in Fig. 6, which illustrate that the room-temperature hardness of the γ' phase increases linearly with molybdenum content. The addition of boron can also strengthen Ni_3Al slightly, because boron atoms occupy interstitial sites and hence produce a lattice distortion. The effect of boron addition on yield and ultimate strengths of this alloy is being studied,[16] and the results suggest that when the boron content is increased from 0 to 0.05 wt.%, the yield strength of the alloy at room temperature and at 870 °C increases by less than 5%. Therefore, the solution hardening of the alloy seems to be mainly due to the addition of molybdenum.

3.3.2 Strengthening by Second Phases

To study the phases present in this alloy at various temperatures, a nickel-aluminum quasi-two-phase diagram with a molybdenum content of 8.2 at.% Mo was constructed. This phase diagram, which is based on a previous study of the Ni-Al-Mo phase equilibria in the temperature range of 600 to 1390 °C,[17-21] is illustrated in Fig. 4. According to this diagram, the second phases appearing in the present alloy at different temperatures are likely to be γNi solid solution, αMo, δNiMo and $\gamma'Ni_3Mo$ phases. The αMo phase was observed in specimens annealed at 1200 to 1240 °C, and its composition (at.%) was determined to be 94Mo-6Ni. The δNiMo phase was observed in specimens aged at 900 to 1100 °C and creep deformed at 1100 °C. The δ phase, the white particles within the grains shown in Fig. 7, forms according to the reaction $\gamma \rightarrow \gamma' + \delta$NiMo and has been identified to have a tetragonal crystal structure.[16] Although the formation of the δ phase leads to a decrease in the γ phase, which is considered to be an important strengthening phase in this alloy, the dispersive distribution of δ phase particles, as shown in Fig. 7, may also act as a strengthening phase, which will partly compensate for the effect of the decrease in γ phase due to the formation of δ phase. The experimental results show that the tensile yield strength of the alloy decreases only by about 10% when specimens are aged for 200 h at 900 to 1100°C.[16] Therefore, it may be considered that these second phases form in different temperature ranges and will have a corresponding strengthening effect at the temperature of their for-

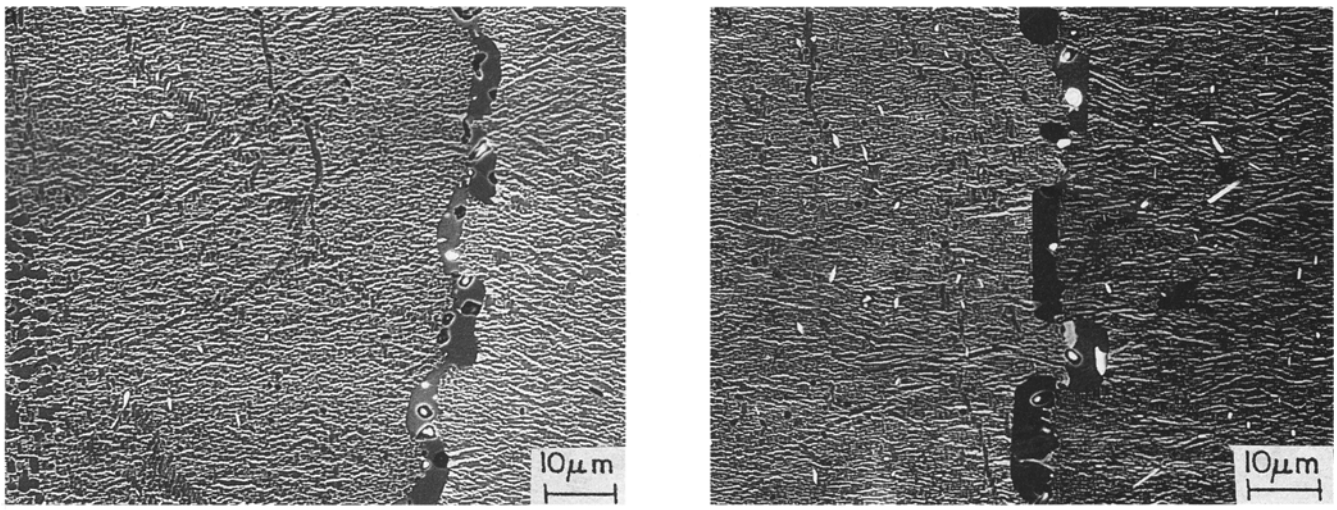

(a) (b) (c)

Fig. 7 Backscattered electron images of microstructures after creep deformation at 1373 K/100 MPa for (a) 30 h, (b) 60 h, and (c) 98 h (ruptured), showing γ raft structure and δ phase.

mation. Therefore, this alloy exhibits excellent mechanical properties over a wide temperature range from room temperature up to 1200 °C.

A small amount (<2 vol%) of borides is also present after the homogenization heat treatment, as shown in Fig. 3. The presence of the borides improves the grain boundary ductility and tensile strength of the alloy. However, it was observed that any increase in boron content beyond 0.05 wt% has a deleterious effect on creep properties of this alloy[16] because of its brittle tetragonal crystal structure and large size (2 to 3 μm) (Fig. 3). Therefore, the boron content in this alloy must be controlled to within 0.03 to 0.05 wt% where the amount of boride is less than 2 vol%.

The γ phase can cause a significant strengthening of the γ′ matrix, as has been reported by Wen et al.[22] They proposed a model to calculate the critical resolves shear stress, Δτ, for an antiphase boundary (APB) dislocation pair to move through the matrix. According to this model, the extra work necessary to pull out dislocation pairs from the precipitate particle is dependent on the difference in the APB energy between the matrix and the precipitate and on the size and volume fraction of the precipitate. The microstructures in Fig. 3 and 5 show that the size of the γ phase is about 200 to 250 Å, which is comparable to the width of the APB dislocation pairs observed in the tensile and creep-deformed specimens of the present alloy. This fine distribution of γ phase with a volume fraction of 0.20 can

have a significant influence on the overall strength of the material.

3.3.3 Strengthening by γ Raft Structure During Creep

The microstructure of this alloy was observed to change significantly during high-temperature creep. Figure 7 shows the backscattered electron images after creep deformation at 1100 °C and 100 MPa for 30, 60, and 98 h. Figures 7(a) and (b) were taken from unruptured specimens, and Fig. 7(c) was taken from a creep-ruptured specimen. Note that the skeletally distributed γ phase that is present after the homogenization heat treatment changed to a raft morphology, which is normal to the applied stress in the interdendrite area, and changed to isolated γ islands in the dendrite arm area. The γ rafts were found to form during the first stage of creep and were stable during the secondary creep stage. From the BSE images, the size of the γ rafts was measured to be about 0.2 to 0.3 μm in thickness and 3 to 5 μm in length. It is believed that, as a barrier to dislocation motion, the raft structure is more effective than the separated γ particles dispersed in the γ′ matrix, because the raft structure may more effectively prohibit the moving dislocations from climbing over the second-phase particles. Consequently, the dislocations move mainly by gliding through from γ to γ′ or γ′ to γ phase. The benefit of the stable raft structure to creep resistance also has been observed in many nickel-base superalloys. Pearson et al. reported that a single-crystal alloy MMT143 (Ni-13Al-9Mo-9Ta, at.%) with the fine and complete γ′ raft structure obtained by special heat treatment and precreep treatment exhibited excellent creep resistance, e.g., the stress-rupture life at 1038 °C and 216 MPa reached 400 to 500 h, which is much longer than all of the current commercial nickel-base single-crystal alloys and the same alloy MMT 143 with coarser, short, and irregular γ′ raft structure.[23] During the tertiary creep stage, the raft structures coarsen and rotate rapidly, which decreases the resistance to dislocation motion and leads to material failure. The coarsening and rotation of γ rafts have been observed in many stress-ruptured specimens, as shown in Fig. 7(c). Therefore, a high regularity and stability of the raft structure will induce a high creep resistance in the alloy. It has been found[10] that the greater the lattice misfit between γ′ and γ, the more stable and regular the raft structure will be as long as the lattice misfit is below a critical value at which coherency is maintained between the γ′ and γ phases. The lattice misfit in the present alloy system has been experimentally determined to be 1.185%, which is higher than most of the present commercial γNi- and γ′Ni_3Al-base superalloys. This may be part of the reason why this alloy exhibits high creep resistance at elevated and intermediate temperature ranges.

3.3.4 Strengthening by Misfit Dislocations

The high yield strengths and creep resistance of this alloy also may be attributed to the high density of misfit dislocation networks at the γ′/γ interface areas due to the high value of the γ′/γ lattice misfit, δ, as shown in Fig. 5. It is obvious that the high density of the misfit dislocation networks can prohibit or retard the movement of dislocations from γ′ to γ or γ to γ′ and hence strengthen the alloy. These regularly arranged dislocations may be considered as predislocation pileups at the γ′/γ interfaces and can be effective barriers to dislocation motion. It was observed that, even in highly deformed specimens from both tensile and creep tests, the density of moving dislocations in the interface area was very low compared to that observed in the γ′ or γ phase, and numerous dislocation pileups were observed at the γ′/γ interface, as shown in Fig. 8.

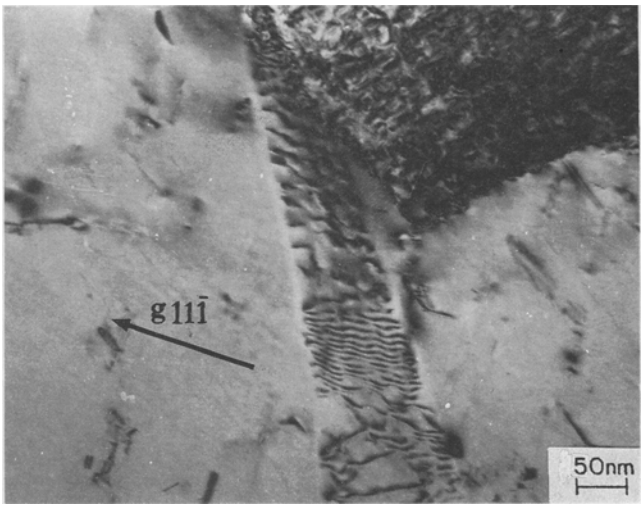

Fig. 8 Dislocation pileups in the front of the γ′/γ interface in a specimen creep deformed at 1373 K/88.3 MPa for 254 h.

4. Conclusions

The high yield strengths from room temperature up to 1100 °C and excellent creep resistance at both intermediate and high temperatures of the present γ′-base superalloy indicate that this alloy is a potential material for turbine blades and vanes of advanced aeroengines. Its superior mechanical properties can be attributed to (1) solid-solution hardening by molybdenum, (2) second-phase hardening by γ, (3) strengthening by the formation of γ raft structure during high-temperature deformation, and (4) strengthening by the present misfit dislocations at the γ′/γ interfaces.

Acknowledgments

The authors wish to acknowledge the Advanced Materials Committee of China and the Natural Science and Engineering Research Council of Canada for their financial support. The authors would also like to express their thanks to Mr. S.H. Li, S. Ma, and Y. Tan for preparing the materials and to W.X. Chen for doing part of the TEM observation.

References

1. K. Aoki and O. Izume, *J. Jpn. Inst. Met.*, Vol 43, 1979, p 1190
2. S.M. Copley and B.H. Kear, *Trans. AIME*, Vol 239, 1967, p 997
3. D.H. Maxwell, *Met. Eng. Quart.*, Vol 10, Nov 1970, p 42
4. S. Chakravorty and D.R.F. West, *Met. Technol.*, Oct 1980, p 414
5. C.T. Liu and V.K. Sikka, *JOM*, May 1986, p 19
6. C.H. Lee, T. Caulfield, and J.K. Tien, *Scri. Metall.*, Vol 21, 1987, p 925
7. J.D. Destefani, *Adv. Mater. Process.*, Vol 2, 1989, p 37
8. P.R. Munroe and I. Baker, *Met. Mater.*, Vol 4, 1988, p 435

9. R.S. Bellows, E.A. Schwarzkoph, and J.K. Tien, *Metall. Trans. A*, Vol 19, 1987, p 479
10. Y.M. Wang, Ph.D. thesis, Institute of Aeronautical Materials, Beijing, China, 1991
11. A. Kelly and R.B. Nickolson, *Strengthening Method in Crystals*, Halsted Press Division, John Wiley & Sons, 1971, p 47
12. H. Brooks, *Metal Interfaces*, American Society for Metals, 1952, p 20
13. M. Dollar and I.M. Bernstein, *Superalloy 1988*, Reichman et al., Ed., The Metallurgical Society, 1988, p 275
14. P. Nash, S. Fielding, and K.R.F. West, *Met. Sci.*, Vol 17, Apr 1983, p 192
15. Y. Mishima, S. Ochiai, M. Yodogawa, and T. Suzuki, *Trans. Jpn. Inst. Met.*, Vol 27, 1986, p 41
16. Y.F. Han and M.C. Chaturvedi, unpublished work
17. R.W. Guard and E.A. Smith, *J. Inst. Met.*, Vol 88, 1959-60, p 283
18. V.Ya Markiv et al., *Akad. USSR Met.*, Vol 5, 1969, p 180
19. L.I. Pryakhina et al., in *Diagrammy Sostoyaniya Metallisch Sistem*, N.V. Aheev, Ed., Moscow, Nauka, 1971, p 112
20. D.B. Miracle, K.A. Lark, V. Srinivasan, and H.A. Lipsitt, *Metall. Trans. A*, Vol 15, 1984, p 481
21. K. Wakashima, K. Higuchi, T. Suzuki, and S. Umekawa, *Acta Metall.*, Vol 31, 1983, p 1937
22. Hui Tian Wen et al., *J. Jpn. Inst. Met.*, Vol 53, Oct 1989, p 1022-1028
23. D.D. Pearson, F.D. Lemkey, and B.H. Kear, *Proc. 4th Int. Symp. Superalloys*, American Society for Metals, 1980, p 513